NASA TECHNICAL MEMORANDUM

NASA TM X-1686

ELECTRICAL STRESS ANALYSIS OF A MICROTHRUSTER POWER CONDITIONER

by Vincent R. Lalli

Lewis Research Center

Cleveland, Ohio

NATIONAL AERONAUTICS AND SPACE ADMINISTRATION • WASHINGTON, D. C. • NOVEMBER 1968

NASA TM X-1686

ELECTRICAL STRESS ANALYSIS OF A MICROTHRUSTER POWER CONDITIONER

By Vincent R. Lalli

Lewis Research Center
Cleveland, Ohio

NATIONAL AERONAUTICS AND SPACE ADMINISTRATION

For sale by the Clearinghouse for Federal Scientific and Technical Information
Springfield, Virginia 22151 – CFSTI price $3.00

ABSTRACT

Obtaining suitable power-conditioning equipment for propulsion experiments is a critical problem. Data obtained on several space projects indicated that failure was caused partly by overstressed electrical parts. A microthruster power conditioner was experimentally analyzed to reveal the problems associated with worst-case overstressed parts. The power conditioner was then modified to eliminate these existing overstressed conditions and has since operated continuously for more than 7000 hours.

ELECTRICAL STRESS ANALYSIS OF A MICROTHRUSTER POWER CONDITIONER

by Vincent R. Lalli

Lewis Research Center

SUMMARY

Obtaining suitable power-conditioning equipment for propulsion experiments is a critical problem. The data presented in this report explain why overstressed electrical parts are a prime cause of this problem. As an example one of the overstressed-part conditions is explained in detail, and the value of experimental stress analysis under worst-case conditions is shown. The example chosen discloses the problems involved when unequal reverse-voltage sharing occurs between rectifiers in high-voltage circuits.

Breakdown theory is used to show that junction deterioration could have been the cause of several critical failures which have occurred during past ion-engine research projects. Further, these breakdown theories are reviewed to show that "avalanche" construction may not be the sole answer to obtaining long-term reliable operation under repeated transient conditions. Evidence is given to show that, for the detailed example chosen, junction deterioration was slowed down by forcing a sharing of the reverse voltage with the addition of a trimmer capacitor at each overburdened exposed junction.

An ion-thruster power conditioner was modified to reflect this trimmer capacitor fix. This power conditioner was further modified to correct other worst-case overstressed conditions and has since operated for more than 7000 hours.

INTRODUCTION

Obtaining suitable power-conditioning equipment for electric propulsion units is widely recognized as a critical problem (ref. 1). Data have been accumulated on several electric propulsion research projects and other power-conditioning development contracts which further show that overstressed electrical parts are a prime cause of equipment failures in electric propulsion experiments.

A typical example of this problem occurred during the WASP fluid dynamic experiment. In this case the failure was in a 28- to 500-volt dc converter which was the power supply for a telemetry transmitter. Failure analysis showed that two, IN 684, submini-

TABLE I. - COMPONENT DERATING FACTORS FOR POWER CONDITIONERS

Component	Derating factor[a]	Component derating weighting factors		Stress	Remarks
		X	Y		
Capacitors				Voltage	The following equation establishes the derating factor for capacitors where values of X and Y are given: Derating factor = $X - \frac{C - C_{min}}{C_{max} - C_{min}}(Y)$ where C capacitance value of capacitor for which derating factor is desired; C_{min} smallest capacitance value available with same case size and voltage rating as C; C_{max} largest capacitance value available with same case size and voltage rating as C
Ceramic disc	0.7	---	---		
Ceramic, low voltage	---	0.5	0.2		
Glass:					
CYFR10 and CYFR15	0.7	---	---		
CYFR20 and CYFR30	.5	---	---		
Porcelain	---	0.7	0.2		
Mica	---	.7	.2		
Plastic film	---	.5	.2		
Paper	---	.8	.1		
Metalized	---	.5	.2		
Tantalum, solid	---	.7	.3		
Tantalum, wet slug and foil	0.7	---	---		
Connectors, low voltage	---	---	---	Current	Contacts shall be derated to 75 percent of rating for individual contacts. The average current rating from 1 to 15 contacts shall be decreased linearly to 20 percent. For more than 15 contacts the rating is 20 percent of the normal individual contact rating. The applied voltage between contacts or between contacts and shell shall not exceed 250 volts rms.
Silicon diodes					Current and voltage derating factors shall be applied simultaneously.
Signal and switching	0.6	---	---	+I	
	.5	---	---	+V, -I	
	.3	---	---	$\overline{W}$	
Power ($I_o \leq 10A$)	.85	---	---	+I	
	.5	---	---	+V, -I	
	.43	---	---	$\overline{W}$	
Power ($10A < I_o \leq 35A$)	.75	---	---	+I	
	.5	---	---	+V, -I	
	.38	---	---	$\overline{W}$	
Zener (power $\leq$ 1W)	.5	---	---	Power	
Zener (1W < power $\leq$ 50W)	.5	---	---	Power	
Microcircuits	---	---	---	-------	Supply voltages may be reduced to effect lower power consumption, at the price of slower switching speeds and narrower noise-immunity margins. Allowable fan-out should be reduced for reliable operation. Operation over wide temperature ranges will generally result in decreased circuit margins and fan-out capability. Operational stability may be improved if power-supply voltage tolerances are tightened, especially if the devices employ non-saturating circuitry.
Relays	0.3	---	---	Current	----------
Resistors				Power	----------
Composition	0.7	---	---		
Film	.4	---	---		
Wirewound power	.5	---	---		
Wirewound precision	.4	---	---		
Transformers	0.4	---	---	Power	----------
Silicon transistors	.25	---	---	Power	Voltage applied across any junction or group of junctions shall not exceed 50 percent of rated voltage.

[a]Derating factor = $\frac{\text{Maximum stress for reliable operation}}{\text{Rated stress}}$

ature silicon rectifiers had shorted out. Experimental measurements showed that the diodes were not carrying equal amounts of the applied reverse voltage. The other ratings for each diode appeared to be reasonable. The fact that these particular diodes were manufactured with avalanche reverse breakdown properties did not seem to be sufficient protection for long-term, reliable operation under these conditions (refs. 2 to 4).

It is generally recognized that component-part failure rates are increasing functions of the stress applied in operation. Furthermore, it is realized that even the best parts, when operated at maximum-rated stress levels, do not have sufficiently low failure rates to allow the synthesis of highly reliable complex systems. Therefore, the need to derate components in application is clearly established (ref. 5).

Component derating factors are naturally based on the component reliability at various stress levels. Once the necessary component reliability is established, the maximum stress level at which the component could be operated can be determined without violating the reliability requirement. Unfortunately, curves of reliability as a function of stress exist for only a few components and are generally not well proven even for these. In the remainder of the cases, historical information based on field data obtained from various equipment operating under conditions similar to those of interest must be used.

Table I shows the recommended derating factors for power conditioners. This table is based on experimental findings and a survey of the best information currently available. Proper use of these derating factors should yield component failure rates in the range 0.1 to 0.001 percent per 1000 hours. Failure rates will also vary widely for different applications because of the particular circuit's tolerance of component drift. Therefore, to ensure low failure rates the designer should strive to achieve the greatest possible circuit tolerance.

This report presents the findings of an investigation made on a microthruster power conditioner to define areas of overstress under worst-case conditions.

SYMBOLS

C capacitance, pF

C_j junction capacitance, F/cm^2

C_t trimmer capacitance, pF

I rectifier current, (+ forward, - reverse), mA

I_{gn} thermally generated electron current, mA

I_{gp} thermally generated hole current, mA

j	equation index
k	Boltzmann constant, ergs/K
N_a	concentration of acceptors, atoms/cm^3
N_d	concentration of donors, atoms/cm^3
n	equation index
P	power, W
P_n	N-region resistivity, Ω-cm
q	electron charge, C
R	reliability
$R_{M, th}$	theoretical reliability of microthruster, dimensionless
$R_{TC, th}$	theoretical reliability of telemetry circuits, dimensionless
T	absolute temperature, K
t	real time, hr
V	rectifier potential (+ forward, - reverse), V
V_A	avalanche potential, V
V_B	barrier potential, V
V_{eq}	equivalent barrier potential, V
$V_{1, 2}$	input potential, V
V_3	negative-charge boundary potential, V
V_4	positive-charge boundary potential, V
$V_{5, 6}$	output potential, V
W	energy rating, W-sec
W_B	barrier width dimension, cm
W_1	negative-charge boundary dimension, cm
W_2	positive-charge boundary dimension, cm
x	crystal dimension, cm
ϵ	dielectric constant, F/cm
θ	phase angle, deg
λ	failure rate, percent/1000 hr
μ_n	electron mobility, cm^2/V-sec

ξ electric field, V/cm

ρ charge density, C/cm^3

σ standard deviation

Subscripts:

i input

max maximum

min minimum

o output

DISCUSSION

An electrical stress analysis test was performed on the microthruster power conditioner while it was operating into an adjustable resistive load bank. (For a more detailed explanation of the apparatus required to operate an ion thruster consult reference 6.) Transient simulation and measurement techniques were worked out. Detailed transient and steady-state data from these measurements are recorded in the microthruster equipment log on file at the Lewis Research Center. These data describe some of the response functions that were observed in the test apparatus under worst-case conditions and help explain why the overstress problems were occurring.

Reliability Model

The Lewis microthruster reliability model with the interconnection arrangement of the circuits with the thruster is shown in figure 1. Each solid-line box is a necessary component of the subsystem. The dashed line defines the subsystem boundaries. The power conditioner has 27 circuits that are operated by a dc power source. These circuits change the primary power into the proper voltage and currents for the thruster heaters, the high-voltage electrodes, and signals of thruster parameters.

Each component has been assigned an identification number or letter corresponding to the equation index n or j. Numbers were used to identify main component blocks. Lower-case letters were used for auxiliary components. Two equations have been added to this diagram that describe (1) the theoretical reliability of the thruster equipment and (2) the theoretical reliability of the telemetry circuits. This diagram was used as

(1) A basis for redundancy

(2) A guide for reliability trade-offs

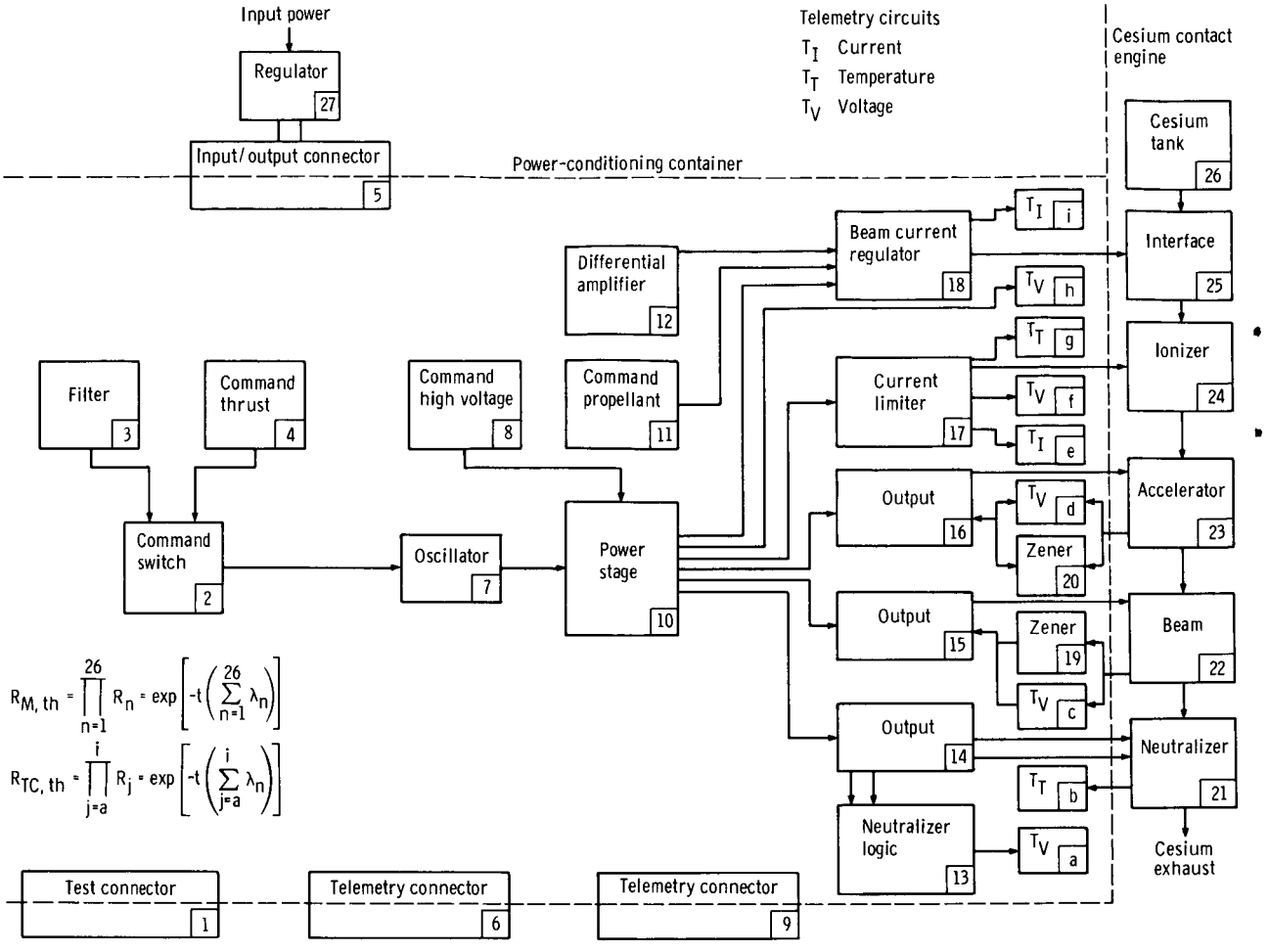

Figure 1. - Microthruster reliability model with identifying devices.

(3) A guide for failure data reporting and analysis

For a more complete treatment of the reliability model consult reference 7.

Summary of Findings

A summary of the worst-case electrical stress analysis findings is given in table II. The parts have been grouped into six categories. The microthruster power-conditioning equipment contained 523 electrical parts; 52 of these parts had not been derated sufficiently to satisfy recommended derating factors. None of these deficiencies were observed either by calculations or under normal operating conditions. It was necessary to investigate various operating conditions experimentally to find the highest stress conditions. Transients caused by turnon, step changes in parameters, simulated arcs, or turnoff were studied in the laboratory to define these problem areas. Each improper

TABLE II. - SUMMARY OF WORST-CASE

ELECTRICAL STRESS ANALYSIS

RESULTS

Component	Total used	Overstressed[a]
Rectifiers	167	26
Transistors	84	9
Capacitors	91	10
Resistors	170	2
Transformers	9	4
Relays	2	1
Total	523	52

[a]Percentage of parts overstressed, 9.9 percent.

TABLE III. - OVERSTRESSED-RECTIFIER

DETAILS

Rectifier, CR	Derating factor[a]	Type	Index (fig. 1)
81, 84, 101	0.80	UTR 62	16
85	1.08	↓	16
89, 93	.93	↓	16
100, 108	1.00	↓	15
109	.63	↓	15
112	.73	↓	15
7	.97	IN 649	2
22	1.74	↓	b
37	5.18	↓	14
113, 114	Spikes	IN 1616	10
54	.97	IN 746	17
8, 9	.79	IN 2999B	10
14, 15	Spikes	FD 300	4
134, 135, 137	↓	↓	11
146, 147	↓	↓	8
165	↓	↓	2

[a]The specified derating factor for working inverse voltage as given in table I is 0.50.

derating condition was analyzed. Corrective design changes were implemented into the breadboard model to eliminate the worst-case overstress conditions.

Although the electrical stress analysis covered the entire microthruster power conditioner, this discussion is limited to one of the more interesting problems, that of the rectifier stresses.

An examination of the data in table III reveals that ten UTR 62 rectifiers were overstressed. All these rectifiers were in output indexes 15 and 16 in figure 1. Three IN 649 rectifiers were found to be overstressed in indexes 2, 14, and b in figure 1. One IN 746, two IN 1616, two IN 2999B and eight FD 300 rectifiers were also overstressed, as shown in table III. In most cases the overstress condition was reverse voltage. In all cases measurements were made for $\pm V$ and $\pm I$ to ensure proper derating under worst-case conditions.

Schematic of Index 15

Experimental data for all the electrical parts were obtained by making electrical measurements on the microthruster power-conditioning breadboard. Index 15 for the beam supply is the voltage quadrupler circuit shown schematically in figure 2. The input forcing function $V_{1,i} = V_{2,i}$ is a regulated -24 volts dc. This voltage is applied through

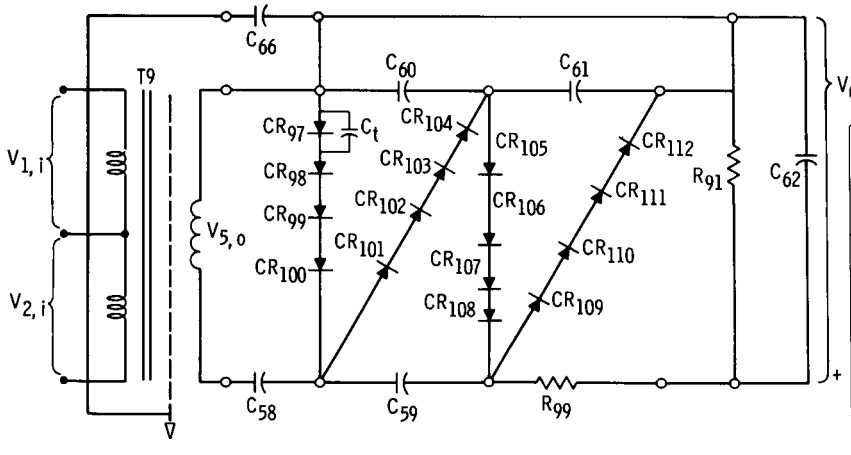

Rectifiers, CR	Trimmer capacitance, C_t, pF
97	27
98	0
99	54
100	156
101	156
102	30
103	0
104	45
105	24
106	0
107	45
108	150
109	72
110	0
111	5
112	60

Figure 2. - Index 15. Output voltage, 1.6 kilovolts dc; maximum output rectifier current, 3.0 milliamperes dc; frequency, 2 kilohertz; input potential, 24 volts dc; $\theta_{1,i} = -\theta_{2,i}$.

an inverter alternately to each half of the primary of T9. The stepped-up output $V_{5,o}$ of T9 is used to charge four quadrupler capacitors, C_{58} to C_{62}, connected through the rectifiers, CR_{97} to CR_{112}, to generate +1600 volts dc output, $V_{6,o}$ (ref. 8). The table in figure 2 shows the final trim capacitance values that were used in the stress-relieved beam supply.

The UTR 62 rectifiers are alloy-diffused silicon devices. The fabrication process is controlled in such a manner as to optimize recovery time. Fast recovery time suggests that an abrupt junction model is appropriate for these devices. This model is used later to show why proper derating for reverse voltage (-V) is important for long-term reliability.

Test Apparatus

The major piece of test equipment used for these observations was an oscilloscope. One of the more interesting test apparatus setups used to measure rectifier voltage is shown in figure 3. A 200 to 1 attenuator and voltage isolation probe was connected to the test specimen. A logarithmic-scale compression circuit was used to measure the rectifier voltages because of its dynamic range of 4 orders of magnitude. The circuit was sensitive to test apparatus loading. The differential probe had an input impedance of 30 megohms and 3 picofarads, which appeared to give minimum circuit disturbance. The

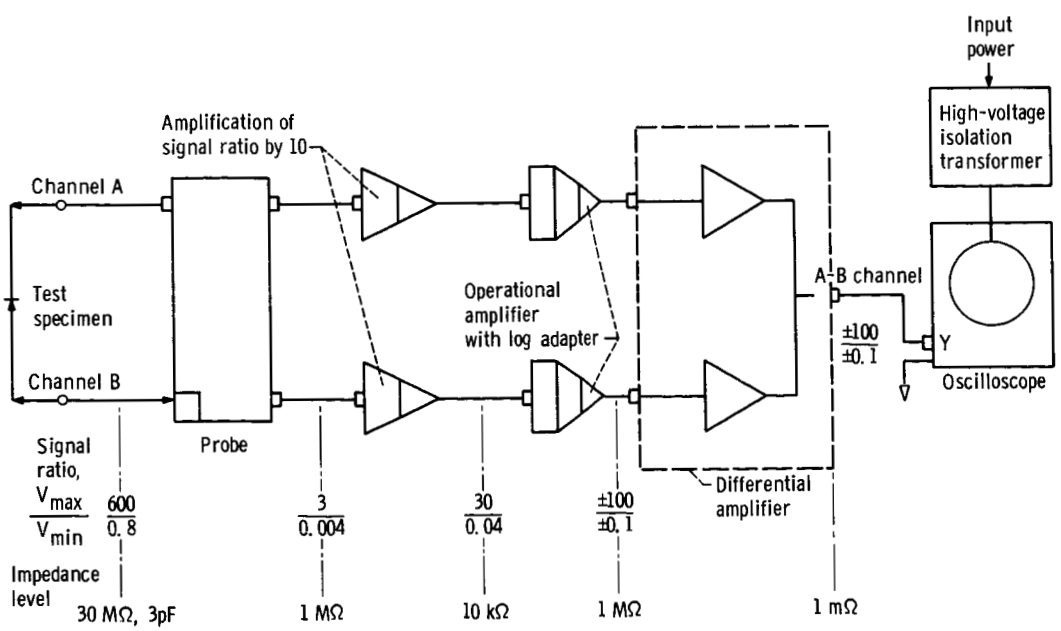

Figure 3. - Apparatus setup for rectifier voltage.

signal ratio V_{max}/V_{min} was reduced from 600/0.8 to 3/0.004 by the probe. This information is amplified by a factor of 10 to 30/0.04 and fed into logarithmic amplifiers for compression. The voltage across the test specimen was obtained by subtracting channel B from channel A. The display device was the oscilloscope.

Ground-loop noises were reduced by connecting the oscilloscope common with the power-conditioner-circuit common and isolating the oscilloscope from its power source.

Unbalance and zero drift are critical adjustments in this dc-coupled measurement technique. Proper attention must be given to each component to assure that it is calibrated, operating, and adjusted properly. Connecting channels A and B to the same point, as a check, assures cancellation of unwanted or interfering signals. It is difficult to resolve ±V beyond about ±10 percent because of scale compression. However, for dynamic measurements on a system with this complexity, greater accuracy was not required.

Experimental Data

Electrical stresses for rectifiers CR_{97} to CR_{112} at laboratory ambient temperature are shown in table IV. The data show that +V, +I, and W meet the requirements of table I. The measured data at laboratory ambient temperature (approx. 21° C) are compared with the specified spacecraft heat sink at a maximum of 60° C to obtain the component derating factor for these conditions. Some of the rectifier diodes have reverse voltage and current stresses, -V and -I, with derating factors of 1.0 and 12.5, respectively, which is considerably above the specified deratings.

A P-N junction is reverse recovered from the forward conducting state when the current passing through the junction goes to zero (i.e., righthand thermally generated hole current I_{gp} equals lefthand thermally generated electron current I_{gn}). For a more complete treatment of the theory of P-N junctions consult references 9 and 10. The junction current goes to zero by diffusion and drift, removing the majority carriers from the junction. At the instant of switching, a current spike occurs which was the cause for $|-I|$ to exceed its dc rating by a factor of about 10. The energy rating of the rectifier is not exceeded by these repetitive reverse-current spikes and is, therefore, not a major concern.

Table IV also shows that the junctions were not sharing reverse voltage equally. The appendix reviews the current theory applicable to junction breakdown to show that equal -V sharing is important for rectifier reliability. For example, CR_{100} would hold off a potential of 600 volts while CR_{98} was carrying only 30 volts peak. Based on these observations, it was clear that reliability could be improved if the diodes shared the reverse voltage more equally. In our example CR_{97} would pick up about five times

TABLE IV. - EXPERIMENTAL CIRCUIT DATA AT LABORATORY AMBIENT TEMPERATURE (21° C)

Rectifier, CR	Rating at 60° C				
	600	1.1 at 1A	1600	0.07 at 600 V	105
	Reverse voltage, -V, volts	Voltage, V, volts	Current, I, mA	Reverse current, -I, mA	Energy rating, W, watt-sec
97	62	0.59	3.8	0.9	0.14×10^{4}
98	30	↓	↓	↓	.07
99	56	↓	↓	↓	.13
100	600	↓	↓	↓	1.4
101	480	.63	8.0	↓	1.1
102	48	↓	↓	↓	.11
103	52	↓	↓	↓	.12
104	240	↓	↓	↓	.55
105	40	.69	20.0	0.8	.08
106	17	↓	↓	↓	.03
107	28	↓	↓	↓	.06
108	600	↓	↓	↓	1.2
109	380	↓	17.0	↓	.76
110	64	↓	↓	↓	.13
111	58	↓	↓	↓	.11
112	440	↓	↓	↓	.88

more -V when CR_{100} shorted out than if CR_{98} shorted out. After a time CR_{97}, which no longer would be properly derated, could fail by this same junction deterioration phenomenon and thereby cause CR_{98} and CR_{99} to carry the remaining burden with no derating. Eventually all rectifiers would fail and the power-conditioner output would go to zero.

Most probably the part with the greatest electrical stresses will fail first. Past experience with diodes has shown that shorting is the dominant failure mode. If some method could be found to make all reverse potentials nearly equal, a derating factor of about 0.33 could be achieved, and the probability of junction deterioration breakdown occurring could be reduced.

Conventional methods (refs. 3 and 4) were employed to improve reverse-voltage sharing as this could possibly have improved the long-term reliability of a series of rectifiers. The circuit stopped operating properly when these different methods were tried.

Recognizing that equal C_j terms should share -V equally, three fixed trim capacitors were added to each string to meet the desired constraint $|0.9\ V| \leq |-V| \leq |1.1\ V|$.

TABLE V. - COMPENSATED, EXPERIMENTAL,

RECTIFIER DATA

Rectifier, CR	Temperature, ^{o}C			
	21		-54 to 85	
	Reverse voltage, -V, peak volts	Reverse current, -I, peak mA	Mean reverse voltage, $-\overline{V}$, peak volts	Standard deviation, σ, peak volts
97	205	1.7	209	5.8
98	200	↓	195	4.7
99	175	↓	172	5.8
100	205	↓	209	4.7
101	190	1.6	195	4.7
102	178	↓	173	7.7
103	170	↓	179	7.7
104	190	↓	198	7.1
105	160	↓	171	7.7
106	162	↓	172	5.8
107	180	↓	183	4.7
108	190	↓	196	5.8
109	192	1.4	201	4.7
110	165	↓	169	4.7
111	160	↓	162	7.7
112	175	↓	179	7.1

In figure 2 the arrangement of trimmer capacitors and their values are shown. Table V shows that quite an improvement in -V has been accomplished by adding the proper C_t without affecting -I appreciably. The maximum spread on uncompensated reverse voltage of 17 to 600 volts peak has been reduced to 160 to 205 volts peak (compare table IV with table V).

Reverse voltage may have exceeded the desired tolerance by a small amount; however, the tolerance was primarily determined by the fixed values of mica capacitors available. Reverse current has been increased roughly by a factor of 2. This is not nearly enough to influence the energy rating W or circuit operating parameters. It remained to show that temperature would not adversely influence voltage sharing and that such a rectifier string would operate for a long time without failure.

Temperature data for $\pm I$ and $\pm V$ were taken by placing the rectifiers, CR_{97} to CR_{112}, and trim capacitors C_t in a temperature chamber. Ten temperatures spaced approximately 14^{o} C apart in the range from -54^{o} to 85^{o} C were selected as test points. The test data for $\pm I$ and $\pm V$ does not show that temperature has any pronounced effect

on the circuit response. Table V summarizes the data for $-V$ by giving the central value $-\overline{V}$ and standard deviation σ in the test temperature range.

The mean value of reverse voltage varies from 162 with $\sigma = 7.7$ volts peak to 209 with $\sigma = 5.8$ volts peak. Further consideration of figure 2 helps explain why temperature has not much influence on voltage sharing for this compensation method. The transformer T9 has been optimized for weight, which tends to increase copper losses; copper, silicon, and mica all have positive changes in resistance, leakage, and capacitance, with temperature. When these two facts are considered, one explanation for this nominal temperature effect may be that as temperature increases the copper losses increase. At the same time the load impedance is decreasing, which tends to maintain a constant response function. Conversely, when temperature decreases the copper losses decrease and the load impedance increases, which tends to hold $V_{6,o}$ constant.

Exhibited Response

The microthruster power-conditioning breadboard revised to eliminate high-stress areas was run in the laboratory without failure for 7052.3 hours.

CONCLUSIONS AND RECOMMENDATIONS

The worst-case electrical stress analysis test performed on a microthruster power-conditioning breadboard disclosed a number of electrical parts which were overstressed. Each overstressed part was analyzed to determine suitable corrective action. Corrective design changes were implemented into the breadboard model.

Experimental measurements showed that a worst-case stress analysis obtained through laboratory testing is necessary to identify overstressed conditions which are not evident from an analytical study or from subjecting the equipment to normal operating conditions. The rectifier diode problem is an example of a worst-case stress condition that was identifiable only through laboratory testing. As a result of this testing, the rectifier problem was solved by adding high-reliability mica capacitors across the rectifiers to improve the voltage sharing capabilities of this design.

Breakdown theory shows that junction deterioration could have been the cause of several critical failures which have occurred on past ion-engine research projects. A further review of these breakdown theories showed that avalanche construction is not always the answer to obtaining long-term reliable operation under a repeated transient condition.

An ion-thruster power conditioner was modified to eliminate the evidenced over-

stressed conditions described herein. This power conditioner operated properly for more than 7000 hours.

Lewis Research Center,
National Aeronautics and Space Administration,
Cleveland, Ohio, August 8, 1968,
704-01-00-17-22.

APPENDIX - JUNCTION BREAKDOWN

Presently there are two theoretical explanations as to how a P-N junction which has voltage applied in the reverse direction abruptly changes from high resistance to essentially zero. Figure 4 shows these two types of breakdown. Both types of breakdown have been observed on an oscilloscope in the laboratory.

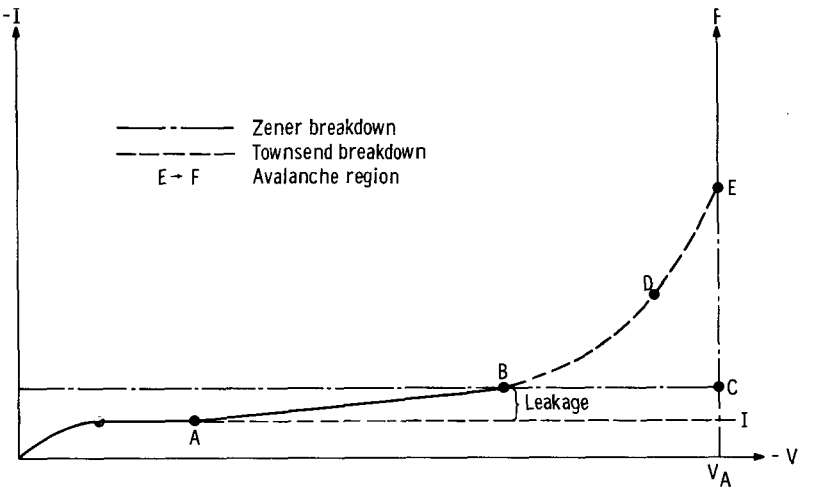

Figure 4. - Steady-state junction breakdown.

From the origin to point A, I appears to be following the theoretical diode equation (ref. 9),

$$I = I_S\left[\exp\left(\frac{qV}{kT} - 1\right)\right] \tag{1}$$

and

$$I_S = I_{gp} + I_{gn}$$

From A to B, I is increased by a leakage component. From B to E, there are two apparent paths by which breakdown occurs. These paths B-C-E and B-D-E are sometimes referred to as the zener and Townsend breakdown paths, respectively. The actual breakdown mechanisms are not well understood as each theory does not fit exactly with the observed phenomena.

The zener breakdown theory (ref. 11) postulates that the covalent bonds in the vicinity of the depletion region are spontaneously disrupted by the high electric fields that

exist in this region. The carriers made available by the disrupted bonds would add to I_{gp} and I_{gn}. For high fields, large numbers of field carriers would be generated, limited only by the external circuit resistance, taking I into the E-F or avalanche region (refs. 12 and 13).

High fields are certainly present in P-N junctions under reverse bias conditions, as can be seen from the following simplified analysis. The experimentally studied rec-

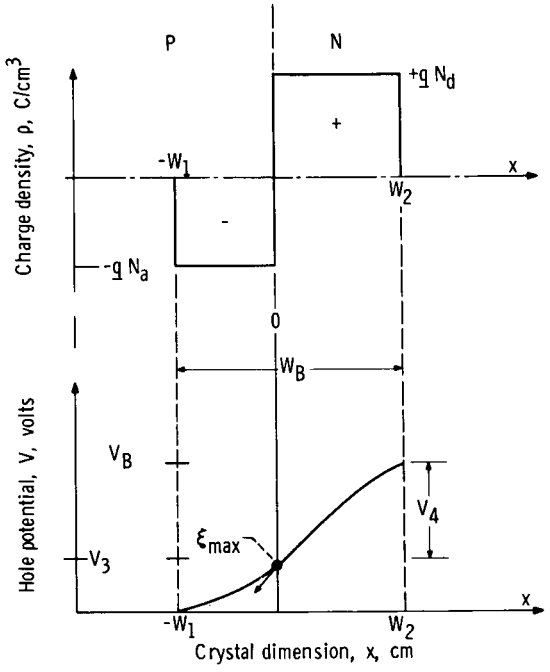

Figure 5. - Abrupt junction model.

tifiers were UTR 62 devices with fast recovery time. Figure 5 shows an abrupt junction model which is appropriate for these devices. Since $x = -W_1 + W_2$ and $\xi = 0$ (fig. 5), a point of inflection occurs at $x = 0$ and ξ is maximum (see ref. 9); therefore,

$$\xi_{max} = \frac{qN_d}{\epsilon} W_2$$

For an abrupt junction,

$$\xi_{max} = \left(\frac{2V_B}{\epsilon \mu_n P_n} \right)^{1/2}$$

For silicon this becomes,

$$\xi_{max} \simeq 6.3\times10^{4}\left(\frac{V_B}{P_n}\right)^{1/2} \tag{2}$$

where

$$P_n = 5.0\ \Omega\text{-cm}$$

$$V_B = V_{eq} - V, \qquad V_{eq} << V$$

Therefore,

$$V_B \simeq |-V| = 200 \text{ volts}$$

and

$$\xi_{max} = 3.98\times10^{5} \text{ volts/cm}$$

Even though this analysis is only approximate, it is clear that this is a very high field and spontaneous disruption of the covalent bonds is quite likely. However, due to the inability of this theory to explain some observable phenomena, it is no longer accepted as complete.

The Townsend breakdown theory (ref. 14) develops the analog between a gas discharge and a P-N junction breakdown. The reverse junction current is composed of thermally generated holes, electrons, and leakage (eq. (1) and fig. 4). When the applied junction potential is increased, from point B, -V increases the energy state to a point where the thermal carriers begin to experience ionizing collisions. Each ionizing collision contributes secondary holes and electrons to -I, beyond the leakage contribution. This causes carrier multiplication to occur, as each ionized carrier may strike several atoms as it passes through the depletion zone. Depending on the magnitude of the applied potential -V, the number of ionizing collisions can cascade quite rapidly as shown along the path B-D-E (fig. 4). From point E upward, the number of carriers generated by collision is no longer a function of -V, as V_A has been reached. The junction current is, in the E-F region, again, only limited by the external circuit resistance.

It can be seen then that all P-N junctions will avalanche at some potential. Whether this disturbance occurs along path B-D-E or B-C-E does not change the fact that this is a very high stress condition for any junction and can easily cause failure. It has been shown in the literature (refs. 2 to 4) that the instantaneous energy rating cannot be ex-

ceeded, or sudden failure by punch-through will occur. The fact that a particular P-N junction can operate in the E-F region under controlled conditions by virtue of avalanche construction does not give total assurance against deterioration due to repeated high reverse-voltage stresses.

Elevating the temperature in which the junction operates aggravates the situation still further. Temperature causes I_S to increase. For silicon, I_S increases about 1 order of magnitude for each 20 K. This increase would suggest that since the number of carriers has increased, the avalanche potential V_A should decrease. Here, both theories appear to be misleading, as in many cases the measured value of V_A increases slightly with temperature.

It appears that the Early effect (ref. 15) under certain conditions may cause deterioration in P-N junctions. This may explain why P-N junctions that were avalanche protected still suffered gradual deterioration as a result of high reverse-voltage stress. This potentially unreliable condition can be minimized by adding a small trimmer capacitor across each exposed junction to cause equalization of reverse voltage.

REFERENCES

1. Anon.: Propulsion. Space/Aeronautics, Res. & Dev. Tech. Handbook, vol. 44, no. 2, 1965-66, p. 49.

2. Hitchcock, R. C.: Avalanche Diodes: The Answer to High PRV. Electronic Design, vol. 12, no. 17, Aug. 17, 1964, p. 166.

3. Gutzwiller, F. W.: Rectifiers in High Voltage Power Supplies. Electronic Design, July 23, 1958.

4. Von Zastrow, E. E.: Voltage Failures in Series-Connected Diodes - Their Cause and Prevention. Electronic Design, vol. 13, no. 22, Oct. 25, 1965, p. 62.

5. Anon.: JPL Preferred Parts List - Reliable Electronic Components. Spec. ZPP-2061-PPL-H. Jet Propulsion Lab., Calif. Inst. Tech., July 1, 1966, table VI.

6. Kotnik, J. Thomas; and Sater, Bernard L.: Power-Conditioning Requirements for Ion Rockets. Presented at the IEEE International Conference and Exhibit on Aerospace Electro-Technology, Phoenix, Arizona, Apr. 19-25, 1964.

7. Lalli, Vincent R.: Ion Engine Subsystem Reliability Procedure. Presented at the IEEE, IES, and ASQC Eleventh National Symposium on Reliability and Quality Control, Miami Beach, Florida, Jan. 12-14, 1965.

8. Smith, Fritz L., ed.: Radiotron Designer's Handbook. Fourth ed., Radio Corp. of America, 1953.

9. DeWitt, David; and Rossoff, Arthur L.: Transistor Electronics. McGraw-Hill Book Co., Inc., 1957.

10. Shockley, W.: The Theory of P-N Junctions in Semiconductors and P-N Junction Transistors. Bell System Tech. J., vol. 28, no. 3, July 1949, pp. 435-489.

11. McAfee, K. B.; Ryder, E. J.; Shockley, W.; and Sparks, M.: Observations of Zener Current in Germanium P-N Junctions. Phys. Rev., vol. 83, no. 3, Aug. 1, 1951, pp. 650-651.

12. McKay, K. G.; and McAfee, K. B.: Electron Multiplication in Silicon and Germanium. Phys. Rev., vol. 91, no. 5, Sept. 1, 1953, pp. 1079-1084.

13. McKay, K. G.: Avalanche Breakdown in Silicon. Phys. Rev., vol. 94, no. 4, May 15, 1954, pp. 877-884.

14. Cobine, James D.: Gaseous Conductors, Theory and Engineering Applications. Dover Publications, 1958.

15. Early, J. M.: Effects of Space-Charge Layer Widening in Junction Transistors. Proc. IRE, vol. 40, no. 11, Nov. 1952, pp. 1401-1406.

NASA-Langley, 1968 — 9 E-4587

NATIONAL AERONAUTICS AND SPACE ADMINISTRATION
WASHINGTON, D. C. 20546

OFFICIAL BUSINESS

FIRST CLASS MAIL

POSTAGE AND FEES PAID
NATIONAL AERONAUTICS AND
SPACE ADMINISTRATION

POSTMASTER: If Undeliverable (Section 158 Postal Manual) Do Not Return

"The aeronautical and space activities of the United States shall be conducted so as to contribute . . . to the expansion of human knowledge of phenomena in the atmosphere and space. The Administration shall provide for the widest practicable and appropriate dissemination of information concerning its activities and the results thereof."

—NATIONAL AERONAUTICS AND SPACE ACT OF 1958

NASA SCIENTIFIC AND TECHNICAL PUBLICATIONS

TECHNICAL REPORTS: Scientific and technical information considered important, complete, and a lasting contribution to existing knowledge.

TECHNICAL NOTES: Information less broad in scope but nevertheless of importance as a contribution to existing knowledge.

TECHNICAL MEMORANDUMS: Information receiving limited distribution because of preliminary data, security classification, or other reasons.

CONTRACTOR REPORTS: Scientific and technical information generated under a NASA contract or grant and considered an important contribution to existing knowledge.

TECHNICAL TRANSLATIONS: Information published in a foreign language considered to merit NASA distribution in English.

SPECIAL PUBLICATIONS: Information derived from or of value to NASA activities. Publications include conference proceedings, monographs, data compilations, handbooks, sourcebooks, and special bibliographies.

TECHNOLOGY UTILIZATION PUBLICATIONS: Information on technology used by NASA that may be of particular interest in commercial and other non-aerospace applications. Publications include Tech Briefs, Technology Utilization Reports and Notes, and Technology Surveys.

Details on the availability of these publications may be obtained from:

SCIENTIFIC AND TECHNICAL INFORMATION DIVISION

NATIONAL AERONAUTICS AND SPACE ADMINISTRATION

Washington, D.C. 20546